THE JOURNAL OF BIOLOGICAL CHEMISTRY VOL. 289, NO. 49, pp. 33971–33983, December 5, 2014
Published in the U.S.A.

Novel RNA-binding Protein P311 Binds Eukaryotic Translation Initiation Factor 3 Subunit b (eIF3b) to Promote Translation of Transforming Growth Factor β1-3 (TGF-β1-3)*

Received for publication, September 5, 2014, and in revised form, October 13, 2014 Published, JBC Papers in Press, October 21, 2014, DOI 10.1074/jbc.M114.609495

Michael M. Yue[‡], Kaosheng Lv[‡], Stephen C. Meredith[‡§], Jennifer L. Martindale[¶1], Myriam Gorospe[¶1], and Lucia Schuger[‡2]

From the [‡]Departments of Pathology and [§]Biochemistry and Molecular Biology, The University of Chicago, Chicago, Illinois 60637 and the [¶]Laboratory of Genetics, NIA, National Institutes of Health, Baltimore, Maryland 21224

Background: P311 is a stimulator of TGF-β1-3 translation, but its mechanism of action is unknown.
Results: P311 binds eIF3b and the 5′UTRs of TGF-β1-3 mRNAs. Thereby, P311 recruits TGF-β1-3 mRNAs to the translation machinery.
Conclusion: P311 is an RNA-binding protein that binds to eIF3b to stimulate TGF-β1-3 translation.
Significance: Our studies add a new level of complexity to TGF-β signaling regulation.

P311, a conserved 8-kDa intracellular protein expressed in brain, smooth muscle, regenerating tissues, and malignant glioblastomas, represents the first documented stimulator of TGF-β1-3 translation *in vitro* and *in vivo*. Here we initiated efforts to define the mechanism underlying P311 function. PONDR® (Predictor Of Naturally Disordered Regions) analysis suggested and CD confirmed that P311 is an intrinsically disordered protein, therefore requiring an interacting partner to acquire tertiary structure and function. Immunoprecipitation coupled with mass spectroscopy identified eIF3 subunit b (eIF3b) as a novel P311 binding partner. Immunohistochemical colocalization, GST pulldown, and surface plasmon resonance studies revealed that P311-eIF3b interaction is direct and has a K_d of 1.26 μM. Binding sites were mapped to the non-canonical RNA recognition motif of eIF3b and a central 11-amino acid-long region of P311, here referred to as eIF3b binding motif. Disruption of P311-eIF3b binding inhibited translation of TGF-β1, 2, and 3, as indicated by luciferase reporter assays, polysome fractionation studies, and Western blot analysis. RNA precipitation assays after UV cross-linking and RNA-protein EMSA demonstrated that P311 binds directly to TGF-β 5′UTRs mRNAs through a previously unidentified RNA recognition motif-like motif. Our results demonstrate that P311 is a novel RNA-binding protein that, by interacting with TGF-βs 5′UTRs and eIF3b, stimulates the translation of TGF-β1, 2, and 3.

P311 is a conserved 8-kDa intracellular protein that neither belongs to an established protein family nor has significant homology with other proteins. P311 is expressed in vascular and visceral smooth muscle beds, the nervous system (1, 2), regenerating tissues, (3–6), and malignant glioblastomas (7). Further, P311 has been shown to induce myofibroblast differentiation and migration (3, 8) and promote nerve and lung regeneration (4, 5). Deletion of *p311* in mice has been reported originally to result in no overt phenotype (9), although these animals displayed learning and memory defects (9, 10). More recently, however, we reported that genetic ablation of P311 leads to decreased vascular smooth muscle cell contractility, hypotonic blood vessels, and vascular hypotension. A defect in TGF-β1, 2, and 3 translation has been identified as the underlying cause responsible for abnormal vascular function (1). Previously, little had been known regarding the processes underlying the regulation of TGF-β translation. To date, the 5′UTR-binding Y-box protein 1 (YB-1), a global translational repressor (11, 12), as well as several microRNAs have been shown to inhibit either TGF-β1 or TGF-β2 translation (11, 13–16). P311 is, therefore, the first documented regulator of all TGF-βs and the only protein currently known to stimulate TGF-β translation *in vitro* and *in vivo*. Because TGF-βs play critical roles in events ranging from fibrogenesis (17) and immunity (18, 19) to cancer (20, 21), we initiated efforts to define the molecular mechanism underlying P311 stimulation of the translation of TGF-β mRNAs.

mRNA translation involves three separate steps: initiation, elongation, and termination (22), with initiation serving generally as the rate-limiting step in this process (23, 24). In eukaryotes, translation initiation begins with the binding of the small (40 S) ribosome subunit to a series of initiation factors, including eIF1, eIF1A, eIF3, eIF5, and the eIF2-GTP-Met-tRNA$_i^{Met}$ ternary complex (TC),[3] to form the 43 S preinitiation complex (PIC). The 43 S PIC then binds to the capped 5′ end of mRNA through eIF4G and the eIF3 complex to scan for the start codon. Following the eIF5-dependent release of eIF2-GDP

* This work was supported, in whole or in part, by National Institutes of Health Grant R01GM111116 (to L. S.). This work was also supported by an award from the American Heart Association (to M. M. Y.).
[1] Supported by the Intramural Research Program of the NIA, National Institutes of Health.
[2] To whom correspondence should be addressed: Dept. of Pathology, The University of Chicago, 5841 S. Maryland Ave., Chicago, IL 60637. Tel.: 773-702-4784; Fax: 773-795-6357; E-mail: lschuger@bsd.uchicago.edu.

[3] The abbreviations used are: TC, ternary complex; PIC, preinitiation complex; IC, initiation complex; SPR, surface plasmon resonance; IP, immunoprecipitation; Ab, antibody; VSMC, vascular smooth muscle cell; RIP, RNA immunoprecipitation; EBM, eIF3b binding motif; aa, amino acid; HLSMC, human lung smooth muscle cell; EV, empty vector; RRM, RNA recognition motif.

and the other eIFs present in the 43 S PIC, the 43 S ribosome subsequently recruits the large (60 S) ribosomal subunit to produce an 80 S initiation complex (IC) containing Met-tRNA$_i^{Met}$ base-paired to AUG in the P site of the ribosome, which is the site where the first aminoacyl tRNA (fMet-tRNA$_f^{Met}$) enters to begin the elongation phase of protein synthesis (23–26).

Of all the initiation factors involved in mRNA translation, eIF3 is the largest and most complex. With a molecular mass of 800 kDa, eIF3 is composed of 13 protein subunits (eIF3a-eIF3m), which are present in stoichiometrically equal amounts (27, 28), with six of the subunits (*i.e.* eIF3a, b, c, e, f, and h) representing core subunits sufficient to support translation initiation (29, 30). eIF3 stimulates most of the reactions in the initiation pathway, including assembly of the eIF2-GTP-Met-tRNA$_i^{Met}$ TC, binding of TC and other components of the 43 S PIC to the 40 S subunit, mRNA recruitment and scanning for AUG recognition and prevention of premature association of 43 S binds to 60 S ribosomal subunits (23, 25, 31, 32). The role of each eIF3 subunit in normal and pathological translation is currently the subject of intense study.

Here we demonstrate that P311 is an intrinsically disordered protein that binds eIF3b and the 5′UTRs of TGF-β1, 2, and 3 mRNAs concomitantly, with little or no binding to other tested 5′UTRs. By directly promoting the enrichment of mRNAs in the translation machinery, P311 enhances TGF-β protein levels. Our findings define P311 as a novel RNA-binding protein as well as one of the few documented eIF3b partners to lie outside of the general translation initiation machinery.

EXPERIMENTAL PROCEDURES

Cell Cultures and Animal Tissues—Mouse NIH-3T3 cells were obtained from the ATCC. NIH-3T3 cells were cultured in DMEM supplemented with 10% (v/v) fetal bovine serum, 100 units/ml penicillin-streptomycin, and 2.5 μg/ml Fungizone. Aortas were dissected from 4-month-old C57BL/6 male mice, and the attached fat and soft tissues were trimmed under a microdissecting microscope. The dissected blood vessels were immediately used for experiments or frozen at −80 °C until use.

Transfection, Gene Silencing, and Reporter Assay—For transient transfections, NIH-3T3 cells at ~70% confluence were transfected with a P311 expression construct, pCMV-MYC-p311, and/or the eIF3b expression construct pCMV-HA-eIF3b (Clontech) using Lipofectamine 2000 reagent in Opti-MEM (Life Technologies). For eIF3b and eIF3a gene silencing, Flexi-Tube GeneSolution siRNAs (targeting four different regions of the *Eif3b* or *Eif3a* gene) (Qiagen) were transfected into cells using Lipofectamine RNAiMAX reagent (Life Technologies). For the reporter assay, TGF-β1-3 5′ and 3′UTRs were cloned into the pGL3-promoter firefly luciferase vector (Promega) to generate reporter constructs (1). NIH-3T3 cells were plated on 6-well plates and transfected with the P311 expression vector, eIF3b siRNA, and the reporter constructs and *Renilla* luciferase internal control vector pRL-SV40. Forty-eight hours after cotransfection, the Dual-Luciferase reporter assay system (Promega) was used to determine the ratio of firefly to *Renilla* luciferase activity, as indicated by the manufacturer.

Protein Purification—To purify full-length eIF3b and fragments from BL21(DE3) *Escherichia coli* (New England Biolabs), a GST tag was fused at the N terminus and expressed in the pGEX-6P-1 vector. The proteins were induced to express in BL21(DE3) cells by 0.4 mM isopropyl 1-thio-β-D-galactopyranoside at 37 °C for 4 h. The *E. coli* cells were then lysed by sonication in 20 mM phosphate buffer (pH 7.5) containing 500 mM NaCl, 1 mM DTT, 0.2% Tween 20, 0.2% Nonidet P-40, and protease inhibitors. Cell lysates were clarified by centrifugation at 4 °C and 13,000 rpm for 30 min. The supernatant was loaded onto a GSTrap column (GE Healthcare). After extensive washes with the lysis buffer, the proteins were eluted in the same buffer containing 10 mM glutathione. The eluted proteins were dialyzed overnight against the binding buffer (25 mM Tris-HCl, 150 mM NaCl, 1 mM DTT, 0.02% Tween 20, 0.02% Nonidet P-40, and 10% glycerol (pH 7.5)). To purify full-length P311 from *E. coli*, a thioredoxin tag and a His$_6$ tag were fused at the N terminus. The protein was purified with a similar method as mentioned above using a HisTrap column (GE Healthcare). While dialyzing overnight against the binding buffer, the thioredoxin tag and the His$_6$ tag were cleaved off with a His$_6$-tagged 3C protease. The cleaved product was further purified by passing through a HisTrap column to remove the tags and the 3C protease.

Surface Plasmon Resonance (SPR)—For analysis of the binding of P311 and eIF3b by SPR, recombinant P311 was immobilized onto the surface of a CM5 (GE Healthcare) sensor chip to ~2000 RU (response units). Purified eIF3b (the GST tag was cleaved) at various concentrations was allowed to flow over the chip, and binding to the P311 was measured by SPR (Biacore 3000, GE Healthcare) with a negative control surface without immobilized P311. The concentrations of eIF3b in the fluid phase were 5, 2, 1, 0.5, and 0 μM in HBS-EP buffer (0.01 M HEPES, pH 7.4, 0.15 M NaCl, 3 mM EDTA, 0.005% v/v Surfactant P20) (GE Healthcare) at 4 °C, respectively.

Co-IP and GST-pulldown—For co-IP, MYC-P311/HA-eIF3b-transfected NIH-3T3 cells were lysed in lysis buffer (25 mM Tris-HCl, 150 mM NaCl, 1 mM DTT, 0.02% Tween 20, 1% Nonidet P-40, and 10% glycerol (pH 7.5)) and clarified by centrifugation at 4 °C and 13,000 rpm for 10 min. The supernatants (1 mg of total protein in a 600-μl volume) were incubated with 20 μl of anti-MYC beads (50% slurry) (Sigma-Aldrich) or 30 μl of anti-HA beads (25% slurry) (Santa Cruz Biotechnology) by rotating at 4 °C for 2 h. After extensive washing three times with 800 μl of lysis buffer, the coimmunoprecipitated proteins were eluted by 20 μl of SDS loading buffer for 10 min at 95 °C and then analyzed by Western blotting. For mass spectrometry, the co-IP material was washed extensively four times with 800 μl of high stringent radioimmune precipitation assay buffer (Pierce). For GST pulldown, the purified GST-eIF3b fragments were incubated with purified P311 in binding buffer on a rocker at 4 °C for 2 h, and then 20 μl of GST beads (25% slurry) (Pierce) was added to the sample. Two hours later, the beads were washed three times with 800 μl of binding buffer, and the proteins on the beads were eluted by SDS loading buffer and analyzed by Western blotting.

Mass Spectroscopy—Proteins were immunoprecipitated from NIH-3T3 cells transfected with MYC-P311 or empty vector using anti-MYC Ab. The immunoprecipitated samples were resolved by SDS-PAGE and digested by trypsin. The trypsinized

samples were analyzed using the Thermo Scientific LTQ Orbitrap LC/MS system. Peptide spectral matching was performed using the Mascot searching algorithm. The results from mass spectrometry analysis are shown in Fig. 1*B*.

Western Blot Analysis—Cell lysates, co-IP/GST pulldown samples, or tissue lysates were resolved on SDS-PAGE gels and transferred onto nitrocellulose membranes (Bio-Rad) for immunoblot analysis. Antibodies against P311 were generated in rabbits by Cocalico Biological, Inc. using bacterially purified P311 as the antigen. Anti-MYC (Sigma-Aldrich), anti-HA Ab, anti-GST Ab, and anti-GAPDH (Santa Cruz Biotechnology) were also used to detect target proteins. An ECL plus Western blotting detection system (GE Healthcare) was used for detecting the chemiluminescence signal.

Immunofluorescence Staining—To detect the colocalization of P311 and eIF3b in VSMCs isolated from aortas (1), cells were cultured on four-chamber slides (Thermo Scientific) until 50% confluence. The VSMCs were then washed three times with 400 μl of PBS and fixed with 4% PFA (paraformaldehyde) for 10 min at room temperature. The fixed cells were permeabilized with 0.2% Triton X-100 for 10 min. After washing extensively with PBS in a 100-ml container, cells were blocked with 3% BSA for 30 min, followed by incubation with primary anti-P311 Ab overnight at 4 °C. After washing, cells were incubated with Alexa Fluor 488 goat anti-rat secondary Ab (Life Technologies) for 1 h at room temperature. Subsequently, cells were blocked and incubated sequentially with anti-eIF3b primary Ab (Abcam), followed by incubation with Alexa Fluor 594 secondary Ab (Life Technologies). Slides were mounted with 50% glycerol containing DAPI for nuclear staining and observed under a Marianas Yokogawa-type spinning disk confocal microscope (Carl Zeiss MicroImaging).

Peptide Synthesis and Competition Assays—P311 peptides (N, M, and C) were chemically synthesized using an ABI 433A peptide synthesizer using Fmoc (*N*-(9-fluorenyl)methoxycarbonyl)-protected aas (Midwest Bio-Tech). Peptides were side chain-unprotected and removed from the resin by TFA treatment in the presence of 2.5% triisopropylsilane, 2.0% anisole, and 0.5% water and then precipitated by addition of diethyl ether. Crude peptides were purified by preparative reversed-phase HPLC using a C18 column. Molecular weights of the final products were determined by mass spectrometry (Bruker UltrafleXtreme MALDI-TOF/TOF). Purified P311 and the GST-eIF3b F4 fragment (10 μM final concentration) were incubated with increasing amounts of synthesized peptides (0, 10, 50, and 100 μM final concentrations) in a final volume of 100 μl of binding buffer. The samples were incubated at 4 °C with gentle rocking, and then GST beads (Pierce) were added to the sample. After washing three times with 800 μl of binding buffer, the supernatants were removed by centrifugation at 3000 rpm for 30 s, and then the beads were boiled for 10 min in 15 μl of SDS loading buffer. Eluted proteins were resolved by SDS-PAGE and then analyzed by Western blotting.

RNA precipitation (RIP)—Forty-eight hours after transfection with P311 expression construct pCMV-MYC-p311 (WT or mutant), eIF3b expression vector pCMV-HA-eIF3b or corresponding empty vectors, the cells were lysed in lysis buffer. Cell lysates were subjected to immunoprecipitation using anti-MYC beads or anti-HA beads as described above. The beads were washed three times in 800 μl of lysis buffer and resuspended in TRIzol (Life Technologies) for RNA isolation. RNAs in the IP materials were detected by RT followed by real-time quantitative PCR using primers specific to TGF-β1 mRNA (sense, 5′-GCT CCC CTA TTT AAG AAC ACC C-3′; antisense, 5′-TTG AGG TTG AGG GAG AAA GC-3′), TGF-β2 mRNA (sense, 5′-AGT GGG AGA GAA AGA GAG AAG G-3′; antisense: 5′-GCG ACC CTA AAA TAG ACC TCT G-3′), TGF-β3 mRNA (sense, 5′-AAG AGA AGC AAG GGA CAG AAG-3′; antisense, 5′-GCT GGG ATG AGG GAT TAT GTA C-3′), and normalization control β-actin mRNA (sense, 5′-CTG TAT TCC CCT CCA TCG TG-3′; antisense, 5′-GCC TCG TCA CCC ACA TAG-3′).

RNA-Protein EMSA—An RNA binding assay was performed according to a previous protocol (33) with modifications. Briefly, single-stranded RNAs were produced by linearizing the pcDNA3.1 plasmid carrying the 5′UTR RNA coding sequences. Transcription was carried out using an *in vitro* transcription kit (RiboMAXTM large scale RNA production system-T7, Promega) in the presence of Ribo m^7G Cap analog (3 mM), and, subsequently, the RNAs were purified using an RNeasy kit (Qiagen) and stored at −80 °C until needed. RNA-protein-EMSA was performed with purified P311 (10 μM) in the presence of increasing amounts (1, 3, 5, and 10 μM) of *in vitro*-translated mRNAs. Binding complexes were resolved in native Tris-glycine gel and detected by Western blotting.

Fractionation of Polyribosomes—Forty-eight hours after transfection, cells were preincubated with cycloheximide (100 μg/ml for 15 min) and lysed with polysome extraction buffer containing 20 mM Tris-HCl (pH 7.5), 100 mM KCl, 5 mM $MgCl_2$, and 0.5% Nonidet P-40. Cytoplasmic lysates were fractionated by ultracentrifugation through 10–50% linear sucrose gradients and divided into 12 fractions. Proteins were analyzed by Western blotting, and RNA was extracted from each fraction using TRIzol (Life Technologies) and used for RT-qPCR analysis.

Statistics—Quantitative data are presented as the mean ± S.D. and were compared statistically by Student's *t* test. $p < 0.05$ was considered statistically significant.

RESULTS

P311 Interacts with eIF3b in an RNA-independent Manner—PONDR® (predictor of naturally disordered regions) analysis (34) suggested that P311 is an intrinsically unstructured protein. CD spectroscopy confirmed the lack of structure in the isolated protein in solution (Fig. 1). Specific ellipticity at all wavelengths measured (260–200 nm) showed a completely linear relationship to protein concentration, indicating that the protein is monomeric under these conditions. As an intrinsically unstructured protein, P311 could acquire tertiary structure by binding to a ligand, *e.g.* another protein (35). To screen for potential binding partners, we performed co-IPs using cell lysates prepared from NIH-3T3 cells expressing MYC-tagged P311 and X-MYC Ab. Mass spectrometric analysis of the co-IP material consistently identified eIF3b as well as several cytoskeletal proteins (Fig. 1*B*). P311-eIF3b interaction was confirmed by co-IP of MYC-P311 and HA-eIF3b, followed by

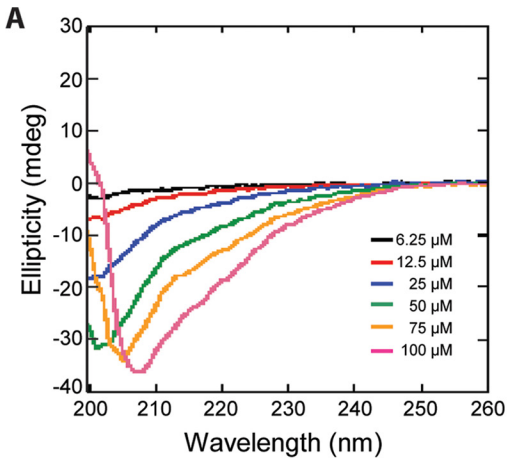

B

Protein	Number of peptides
P311 (NREP)	38
MYH9	15
ACTB	8
EIF3B	8
FLNA*	6
GDI2	3
RAB7	3
EIF3G	2
RPS13	2
RBMX	1

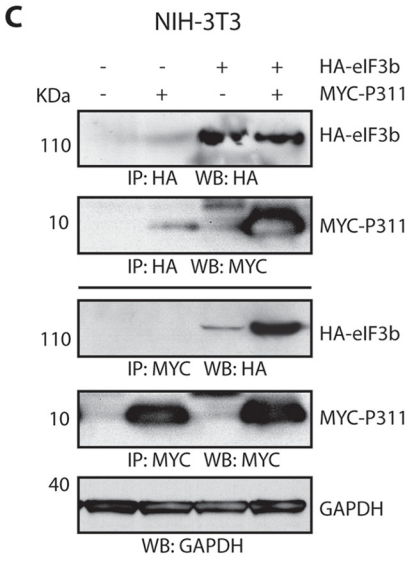

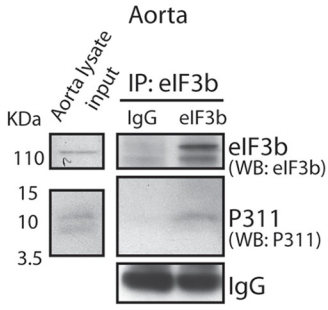

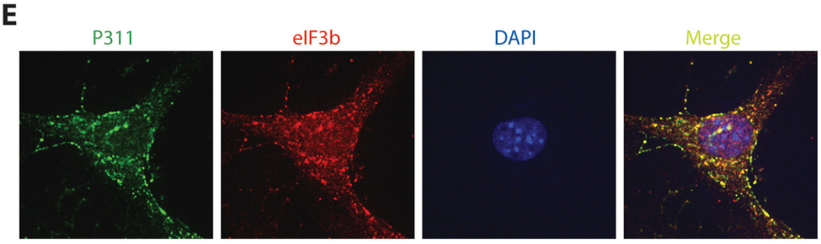

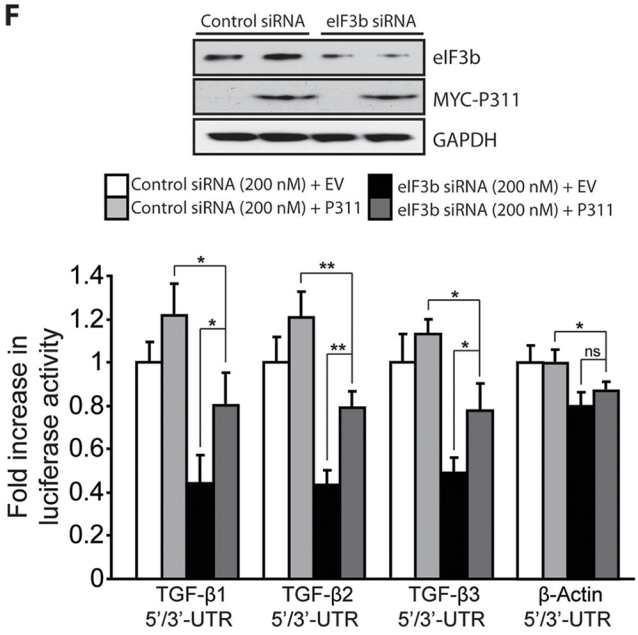

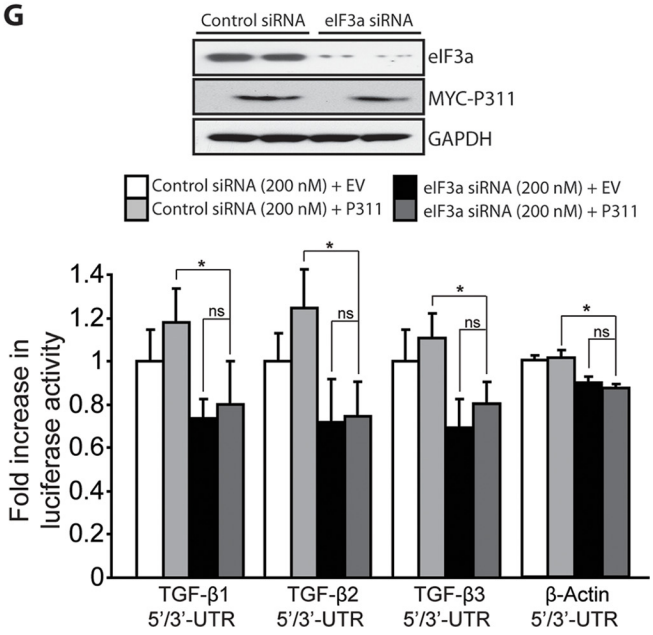

immunoblot analysis using X-MYC and X-HA Abs (Fig. 1*C*). Interaction of endogenous P311 and eIF3b was demonstrated by immunoblot identification of P311 in co-IPs performed with X-eIF3b Ab on lysates of mouse aortic smooth muscle (Fig. 1*D*) and by confocal microscopy, revealing their colocalization in VSMCs (Fig. 1*E*).

Because the eIF3 complex binds different types of RNA (36, 37), we tested whether the P311-eIF3b interaction might be RNA-mediated by treating the samples with RNase prior to co-IP. Samples without RNase treatment were used as controls. The co-IP material was washed and resolved by SDS-PAGE. No change was observed in P311-eIF3b binding in the absence of RNA (data not shown).

eIF3b-P311 Interaction Does Not Affect the Level and Composition of eIF3b-associated Subunits—Immunoblot analysis of eIF3b IP material with the appropriate Abs showed no significant difference in the levels and composition of eIF3b and eIF3b-associated subunits (eIF3a, g, i, and j) in the presence or absence of P311, indicating that P311 does not serve as an intermediary to recruit eIF3b-associated subunits to the eIF3 complex (data not shown).

eIF3b-P311 Interaction Is Required for P311-induced Translation of TGF-β—eIF3b or eIF3a were silenced by RNAi (Fig. 1, *F* and *G*) in the presence or absence of P311, and then RNA reporter assays were performed using TGF-β 5/3′UTR expression vectors (1). Upon eIF3b down-regulation, the absence of P311 decreased TGF-β translation more dramatically than when P311 was present (Fig. 1*F*). Upon eIF3a down-regulation (negative control), no significant difference was observed between the absence and presence of P311 on TGF-β translation (Fig. 1*G*). Together, these results indicate that eIF3b is required for P311-controlled TGF-β translation, whereas eIF3a is not.

P311-eIF3b Interaction Is through Direct Binding—GST pulldown assays were performed using purified recombinant P311 and GST-eIF3b with GST as a negative control. As shown in Fig. 2*A*, GST-eIF3b, but not GST, bound to P311. SPR was used to examine whether there is direct P311-eIF3b binding. After removing the GST tag from the recombinant eIF3b (Fig. 2*B*), P311 was immobilized on a BIAcore sensor chip, and various concentrations of eIF3b were allowed to flow over the chip while the interaction of P311 with eIF3b in the mobile fluid phase was monitored. A BIAcore sensor chip without immobilized P311 served as a negative control. The SPR study confirmed direct P311-eIF3b interaction with a K_d of 1.26 μM and 1:1 (mol:mol) stoichiometry. (Fig. 2*B*).

P311-eIF3b Binding Is Mediated by the eIF3b RRM and the Conserved P311 eIF3b Binding Motif (EBM)—A series of GST-eIF3b fragments was generated for GST pulldown studies (Fig. 2*C*). Only the full-length eIF3b (*FL*) and an N-terminal fragment encompassing the eIF3b RRM fragment (*F2*) were able to bind to P311 (Fig. 2*D*). By testing each half of the F2 fragment (*F3* and *F4*), F4, representing the eIF3b RRM, was identified as the binding site for P311 (Fig. 2*E*).

P311 was divided into three segments of similar length: N-terminal (amino acid (aa) residues 1–22), referred to as N segment; middle (aa residues 23–46), referred to as M segment; and C-terminal (aa residues 47–68), referred to as C segment (Fig. 3*A*). Peptides representing each of these three segments (referred to as N peptide, M peptide, and C peptide) were chemically synthesized and used to perform GST-F4 gel motility shift assays with GST as a negative control. A shift in F4 motility was observed when incubated with the M peptide but not with the other two (Fig. 3*B*). Competition assays showed that addition of M peptide reduced P311 binding to F4 in a concentration-dependent manner, whereas N and C peptides had no effect (Fig. 3*C*).

To further demarcate the eIF3b binding site within the P311 M segment, we searched for conserved P311 aa sequences among higher eukaryotic species. This analysis revealed the presence of a highly conserved 11-aa-long stretch (from leucine 30 to lysine 40) within the middle region of P311 (Fig. 3*D*, *stars*). A series of tandem mutations in the conserved region were generated by alanine substitutions (Fig. 3*D*). The P311 mutants were coexpressed together with HA-eIF3b, followed by co-IPs with X-HA Ab. The mutant in which alanine residues were substituted for all 11 aas inhibited P311-eIF3b binding by 95% (Fig. 3*E*). Therefore, this 11-aa sequence was designated as an EBM and its mutant as P311(Mut^{EBM}) (Fig. 3*E*). *In vitro* binding assays were performed to confirm the involvement of this region. Recombinant GST-F4 was incubated with MYC-P311 or MYC-P311(Mut^{EBM}), each of them bound to X-MYC Ab-conjugated beads. After extensive washing, the material bound to the beads was examined by Western blotting using X-GST Ab. As shown in Fig. 3*F*, the eIF3b F4 fragment bound to P311, whereas no binding was observed between F4 and P311(Mut^{EBM}).

The EBM Is Required for P311 Induction of TGF-β Translation and for a P311-mediated Increase in the Levels of TGF-β in Human Lung Smooth Muscle Cells (HLSMCs)—Polysome fractionation analysis of NIH-3T3 cells expressing P311 or P311(Mut^{EBM}) was performed. The majority of P311, but not P311(Mut^{EBM}), β-actin, or GAPDH, cosedimented with eIF3b

FIGURE 1. **P311 interacts with eIF3b.** *A*, P311 is an unstructured protein. Purified recombinant P311 at different concentrations was analyzed by CD. *mdeg*, millidegrees. *B*, summary of the mass spectrometry analysis. MYC-P311 and potentially interacting proteins were coimmunoprecipitated from NIH-3T3 cells transfected with MYC-P311 or empty vector using anti-MYC Ab. The coimmunoprecipitated samples were analyzed by mass spectroscopy using the Thermo Scientific LTQ Orbitrap LC/MS system. Peptide spectral matching was performed using the Mascot searching algorithm. *C*, Co-IP of HA-eIF3b and MYC-P311 from NIH-3T3 cells transfected with either of them alone or in combination. After 48 h, the cells were lysed, and the lysates were used for IP with the indicated antibodies. IP material was resolved by SDS-PAGE, transferred to membranes, and immunoblotted with the indicated antibodies. *WB*, Western blot. *D*, co-IP of endogenous eIF3b and P311 from mouse aortic smooth muscle lysate using the indicated antibodies. *E*, confocal microscopic colocalization of immunostained P311 and eIF3b in VSMCs. *F*, luciferase reporter assay for TGF-β 5′/3′UTRs in NIH-3T3 cells transfected with P311 or EV while eIF3b is concomitantly down-regulated by siRNA or exposed to scrambled siRNA control. *G*, luciferase reporter assay for TGF-β 5′/3′UTRs in NIH-3T3 cells transfected with EV or P311 while eIF3a is concomitantly silenced by siRNA or exposed to scrambled siRNA control. In *F* and *G*, eIF3b and eIF3a were silenced by siRNAs targeting four different regions of the *Eif3b* and *Eif3a* genes, respectively. A final concentration of 200 nM was used. *, $p < 0.05$; **, $p < 0.01$.

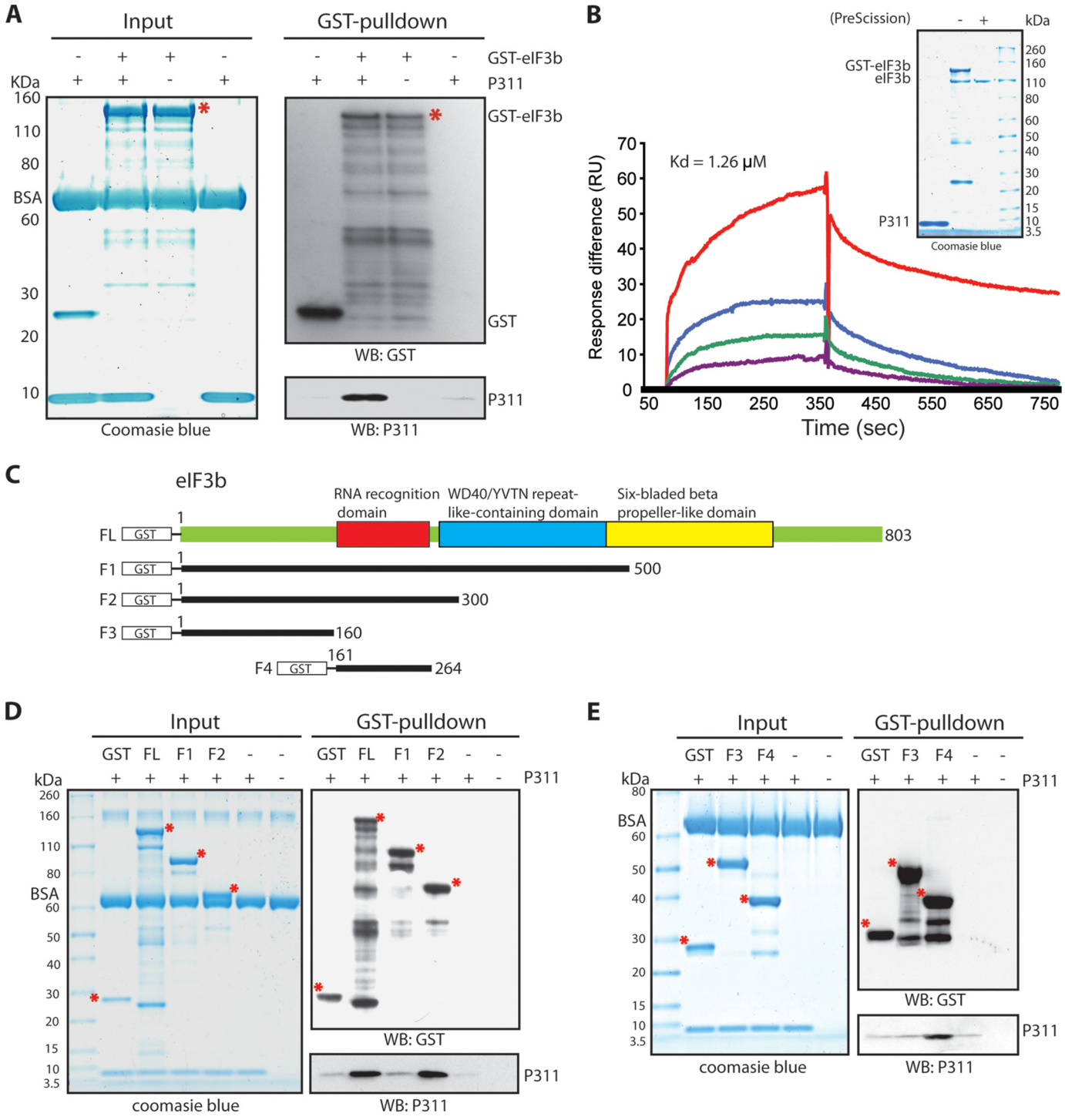

FIGURE 2. **P311 directly binds to the eIF3b RRM.** *A*, GST pulldown assays using bacterially expressed recombinant GST-eIF3b and P311. GST-eIF3b was incubated with or without P311, followed by addition of GST beads. After extensive washing, the proteins bound to the GST beads were separated by SDS-PAGE and detected with anti-GST or anti-P311 Ab. The input recombinant proteins were separated by SDS-PAGE and visualized with Coomassie Blue staining. BSA was added as a nonspecific competitor. The *asterisks* indicate the main bands of input of full-length GST-eIF3b. *WB*, Western blot. *B*, analysis of P311-eIF3b binding by SPR. Recombinant P311 was immobilized onto the surface of a CM5 sensor chip to ~2000 RU. Various concentrations of purified eIF3b (after removal of the GST tag) were allowed to flow over the chip, and binding to the P311 was measured by SPR with a negative control surface devoid of P311. The concentrations of eIF3b in the fluid phase were 5, 2, 1, 0.5, and 0 μM, respectively. *C*, eIF3b and its fragments used in the following studies. Each fragment was fused with a GST tag at the N terminus for protein purification and GST pulldown using GST beads. *FL*, full-length. *D* and *E*, binding of eIF3b RRM to P311. Recombinant GST tag alone, GST-full-length eIF3b (*FL*), and GST-eIF3b fragments (*F1*, GST-eIF3b 1–500 aa; *F2*, GST-eIF3b 1-300 aa; *F3*, GST-eIF3b 1–160 aa; *F4*, GST-eIF3b 161–264 aa) were incubated with purified P311, followed by addition of GST beads. After washing, the proteins were released from the beads in SDS gel loading buffer and analyzed by Western blotting. An aliquot of the binding reaction was analyzed separately by SDS-PAGE and stained with Coomassie Blue as input (*left panels*). BSA was added to all reactions as a nonspecific competitor. The *asterisks* indicate the main bands of input GST-eIF3b fragments.

and 40 S ribosome (Fig. 4*A*). A portion of P311 was found to be cosedimenting with small and large polysomes (fractions 6–10), suggesting that P311 might associate with mRNA present in polysomes. To determine whether the mRNAs encoding TGF-βs were present in the same fraction as P311, we analyzed their relative distribution in the gradients (Fig. 4*B*). Compared

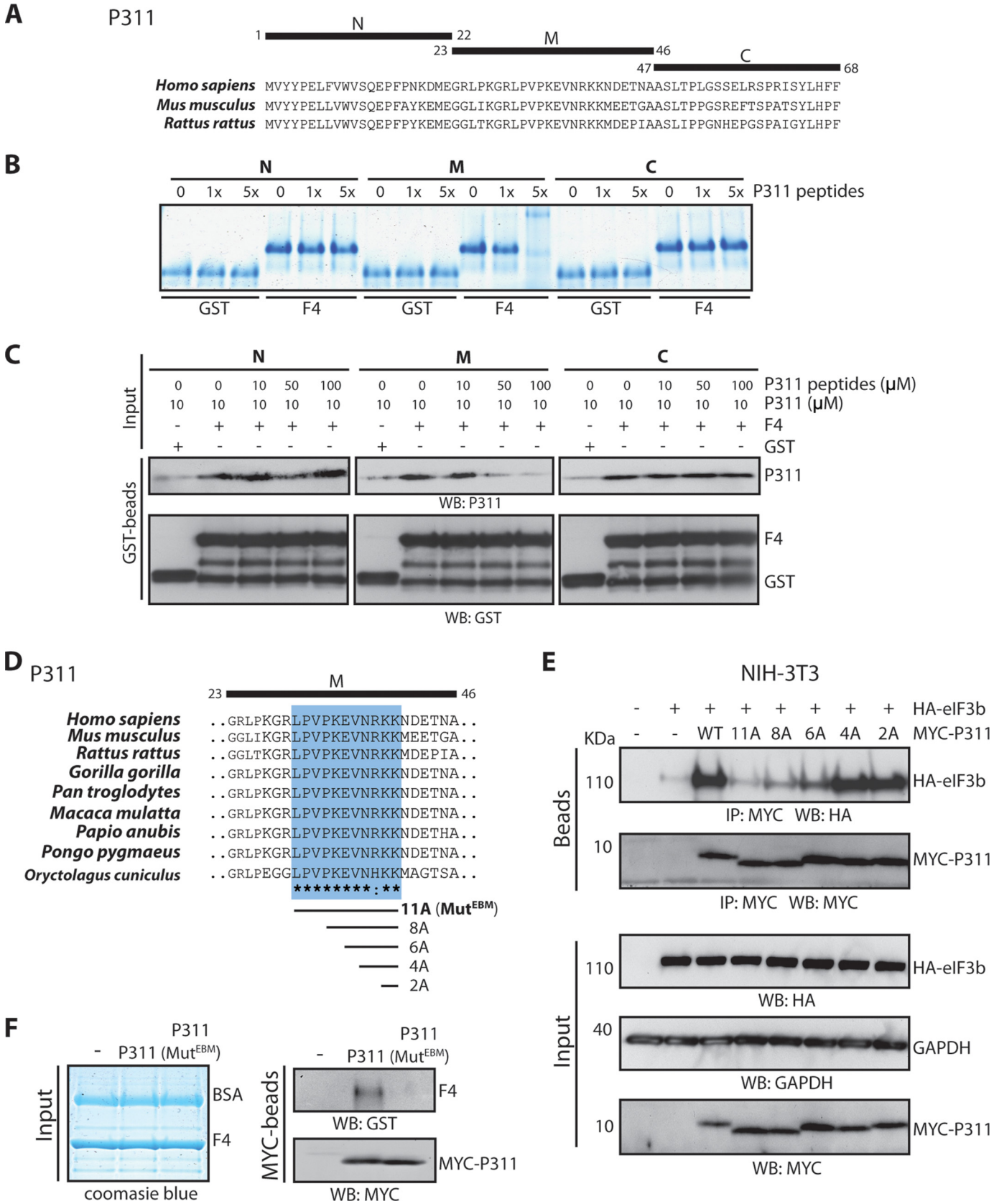

with the distribution of TGF-β1 mRNA in empty vector (EV)-transfected control cells (Fig. 4*B*, *green curve*, peaking at fraction 8–9), overexpression of P311 shifted the TGF-β1 mRNA to higher gradient fractions (mainly fraction 10), consistent with the increase in TGF-β1 mRNA translation in P311-transfected cells. In P311(Mut^{EBM})-transfected cells, the shift of the peak at fraction 10 was reduced significantly (Fig. 4*B*, *blue curve*, peaking at fractions 8 and 10). Similar distributions were seen for TGF-β2 and 3 (Fig. 4*B*). The distribution of the β-actin mRNA control largely overlapped among EV-, P311-, and P311(Mut^{EBM})-transfected cells (Fig. 4*B*). The recruitment of TGF-β RNAs to the eIF3 complex by either P311 or P311(Mut^{EBM}) was determined by RIP assays. HA-eIF3b and MYC-P311 or MYC-P311(Mut^{EBM}) were cotransfected to NIH-3T3 cells. eIF3 subunits were then cross-linked by dimethyl 3,3′-dithiobispropionimidate · 2 HCl, a cleavable cross-linker that stabilizes adjacent protein-protein interactions (38), prior to IP of the eIF3 complex with an X-HA Ab. These studies showed greater enrichment in TGF-β mRNAs in the eIF3 complex from cells expressing P311 than in cells expressing P311(Mut^{EBM}) (Fig. 4*C*). Finally, reporter assays using the 5′/3′UTR constructs of the three TGF-β isoforms showed decreased luciferase activity in NIH-3T3 cells transfected with P311(Mut^{EBM}) compared with P311 (Fig. 4*D*).

As expected from studies presented in Fig. 4, ELISA demonstrated that P311(Mut^{EBM}) failed to increase TGF-β1-3 levels in HLSMCs (Fig. 5*A*). Consistent with the role of P311 in TGF-β1-3 translation, the levels of the corresponding mRNAs were unchanged (Fig. 5*B*).

P311 Binds to the 5′UTRs of TGF-β mRNAs through a Conserved P311 RRM-like Signature Motif—Although Blast and searches in the database of European Molecular Biology Laboratory-The European Bioinformatics Institute (EMBL-EBI) of the P311 aa sequence failed to identify functional motifs, a recent analysis using BindN with 90% specificity (39) predicted a conserved RRM-like signature consisting of 13 positively charged aas (Fig. 6*A*, *arrowheads*) partially overlapping with the EBM (Fig. 6*A*). To determine whether P311 directly binds to TGF-β mRNAs, NIH-3T3 cells transfected with MYC-P311 or EV were exposed to UV light to specifically stabilize protein-RNA interaction (40). This was followed by RIP using X-MYC Ab. These studies showed that P311 directly binds to TGF-β mRNAs (Fig. 6*B*). The binding to TGF-β mRNAs was largely decreased when expressing the P311(Mut^{RRM}) (all 13 potential RNA-binding sites mutated to alanine), with no significant effect on other control mRNAs. *In vitro* RNA-protein binding assays followed by RNA-protein EMSA were performed using recombinant P311, P311(Mut^{RRM}) and *in vitro*-produced 5′UTRs from several mRNAs, including those that encode TGF-βs, GAPDH, β-actin, 18 S rRNA, and the protein product of the TGF-β1 neighboring gene B9d2. All RNAs were confirmed to be effective in protein binding using as a control eIF4E, an established RNA-binding protein (41, 42) (data not shown). The interaction of P311 with increasing concentrations of these various RNAs was observed by RNA-protein EMSA (Fig. 6*C*). The relative density of bound P311 signal was analyzed using ImageJ software, which indicated that P311 binds to the 5′UTR of TGF-β mRNAs with a significantly higher affinity than to all the controls RNAs tested (Fig. 6*D*).

DISCUSSION

P311 was discovered more than two decades ago (2), but its biological importance has only been revealed recently in studies demonstrating its stimulatory effects on TGF-β1-3 translation and, therefore, on blood pressure regulation (1). Because TGF-βs play key roles in multiple pathophysiological processes, we directed further efforts toward understanding the molecular mechanisms by which P311 regulates TGF-β mRNA translation.

We found that P311 is intrinsically unstructured. Therefore, it could require a binding partner to acquire tertiary structure and function (35). Hence, we employed transfected NIH-3T3 cells, which do not express P311 (3), as well as P311-expressing VSMCs (1) to search for P311 binding proteins with potential involvement in mRNA translation. Our studies led to the identification of eIF3b, a subunit of the multicomplex translation initiation factor eIF3 (43), as a direct binding partner of P311.

In co-IP mass spectrometry studies, P311 also showed an association with several cytoskeletal proteins, including filamin, previously reported to interact with P311 (44), myosin heavy chain, and β-actin, suggesting that, besides the stimulation of translation of TGF-β1-3, another P311 function may be to link TGF-β transcripts to molecular motors for active transport (45). The previously observed binding of P311 to the TGF-β1 latent associated protein by two-yeast hybridization and co-IP (46) was not seen in this study. One of the reasons for this discrepancy could be that, in the previous study, latent associated protein was introduced into NIH-3T3 cells by digoxigenin permeabilization of the cellular membrane before performing co-IP, a method which may have led to a large increase of intracellular latent associated protein, facilitating its interaction with P311.

eIF3, the largest eIF complex, is composed of 13 subunits, named eIF3a to eIF3m (30). Several of them have been identified as core subunits (47). eIF3b is one of them, whereas the others are eIF3j, eIF3a, eIF3g, eIF3i, and eIF3e (25, 48). These

FIGURE 3. **A conserved P311 aa sequence is required for eIF3b binding.** The sequence is referred to as EBM. *A*, aa sequence alignment of P311 from different species using ClustalW. Identical aas, similar aas, and nearly similar aas are shown underneath the sequences as *stars*, *single dots*, or *double dots*, respectively. N, N-terminal (1–22 aa); M, middle (23–46 aa); C, C-terminal (47–68 aa). *B*, gel mobility shift assay performed with purified GST-eIF3b F4 (shown in Fig. 2*C*) in the absence or presence of increasing amounts of synthesized N, M, and C P311 peptides. After incubation, the proteins were resolved on a 4–20% Tris-glycine native gel, followed by Coomassie Blue staining. *C*, competition assay performed by GST pulldown using equal amounts of purified GST-F4 incubated with 10 μM purified P311 in the in the presence or absence of increasing concentrations of synthesized P311 peptides (10, 50, and 100 μM). The resulting Western blots (*WB*) were probed with the indicated antibodies. *D*, a conserved P311 region among different species. Tandem mutations were made for the following experiments. *E*, lysates from NIH-3T3 cells expressing either MYC-P311 with or without the indicated mutations and HA-eIF3b were subjected to IP and Western blotting. *F*, equal amounts of the recombinant GST-eIF3b F4 were incubated with the MYC-beads bound with MYC-P311 or MYC-P311(Mut^{EBM}). Proteins were released from the beads in SDS-PAGE loading buffer and analyzed by Western blotting.

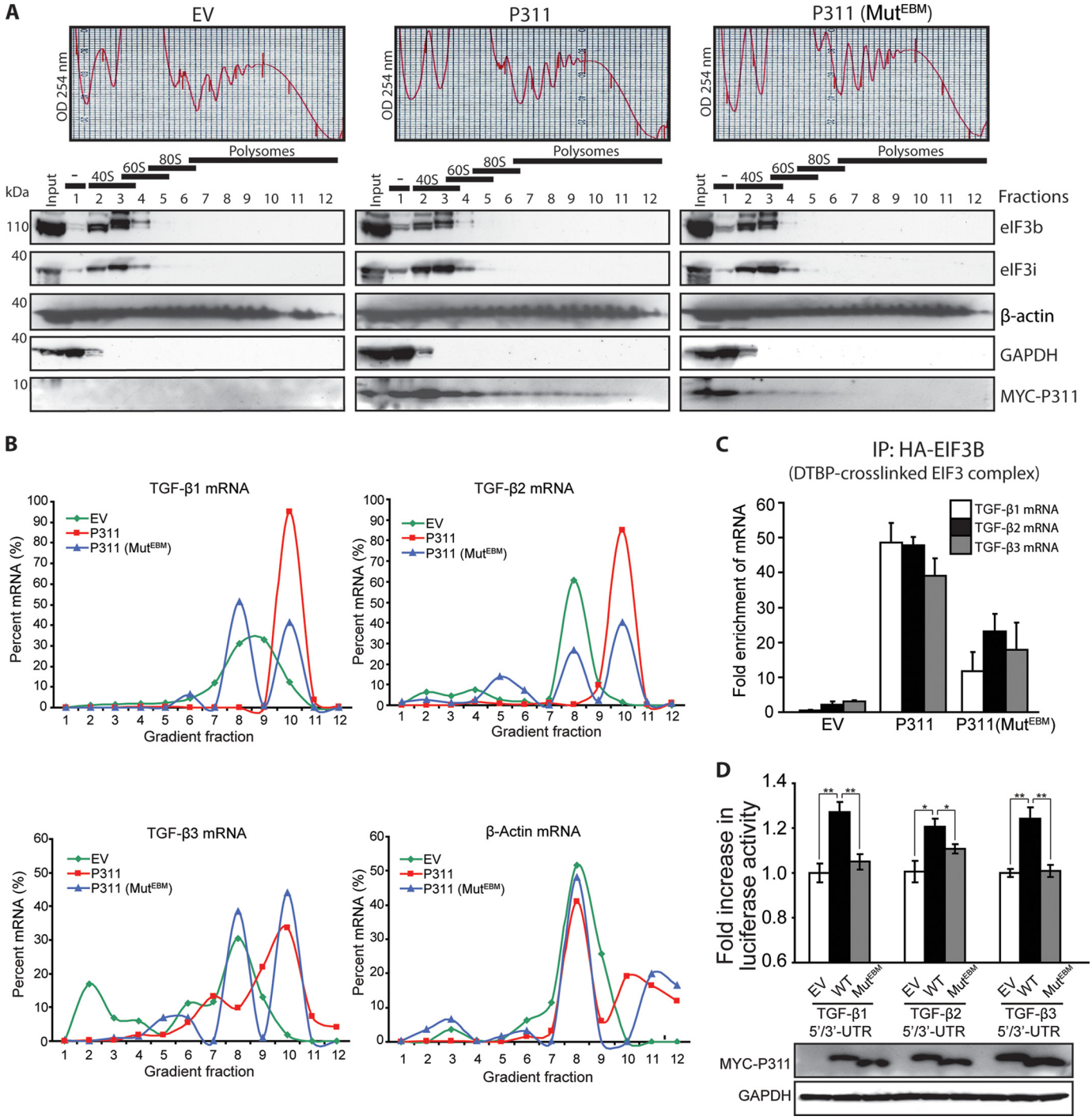

FIGURE 4. **The EBM is required for P311 induction of translation of TGF-β1-3.** *A*, cytoplasmic extracts from EV-, P311-, and P311(Mut^{EBM})-expressing cells were fractionated through sucrose gradients, with the lightest components sedimenting at the top (fraction 1); small (40 S) and large (60 S) ribosomal subunits and monosomes (80 S) in fractions 2–6; and progressively larger polysomes, ranging from low to high molecular weight, in fractions 6–12. Proteins on polysome gradients were detected by Western blotting. −, no ribosomal components; *OD*, optical density. *B*, polysome analysis of TGF-β1-3 mRNAs. The relative distribution of TGF-β1-3 mRNAs and β-actin mRNA on polysome gradients was studied by RT-qPCR analysis of the RNA present in each of 12 gradient fractions and is represented as percent of total mRNA. *C*, RIP assay showing enrichment in the 5′UTRs of TGF-β mRNAs in the eIF3 IP from cells transfected with EV, P311, or P311(Mut^{EBM}). eIF3 complexes were subjected to IP through HA-eIF3b, and the subunits were detected using the corresponding antibodies. RNA enrichment was detected by RT-qPCR. *D*, luciferase reporter assays for TGF-β 5′/3′UTRs in NIH-3T3 cells transfected with EV, P311, or P311(Mut^{EBM}). *, $p < 0.05$; **, $p < 0.01$.

core subunits are necessary and sufficient to initiate translation (47, 49–51).

Although eIF3b is highly expressed in several forms of cancer (52–55) and its down-regulation has been shown to inhibit the proliferation and metastatic potential of colon, bladder, and prostate cancers (52, 53), little is known about eIF3b function(s) at the molecular level. Previous research indicated that eIF3b serves as a binding scaffold for the other core subunits and for eIF2 (47, 49–51), whereas its interaction with eIF3a, eIF3j, and eIF1a ensures proper formation of the scanning-arrested conformation required for stringent AUG recognition (56).

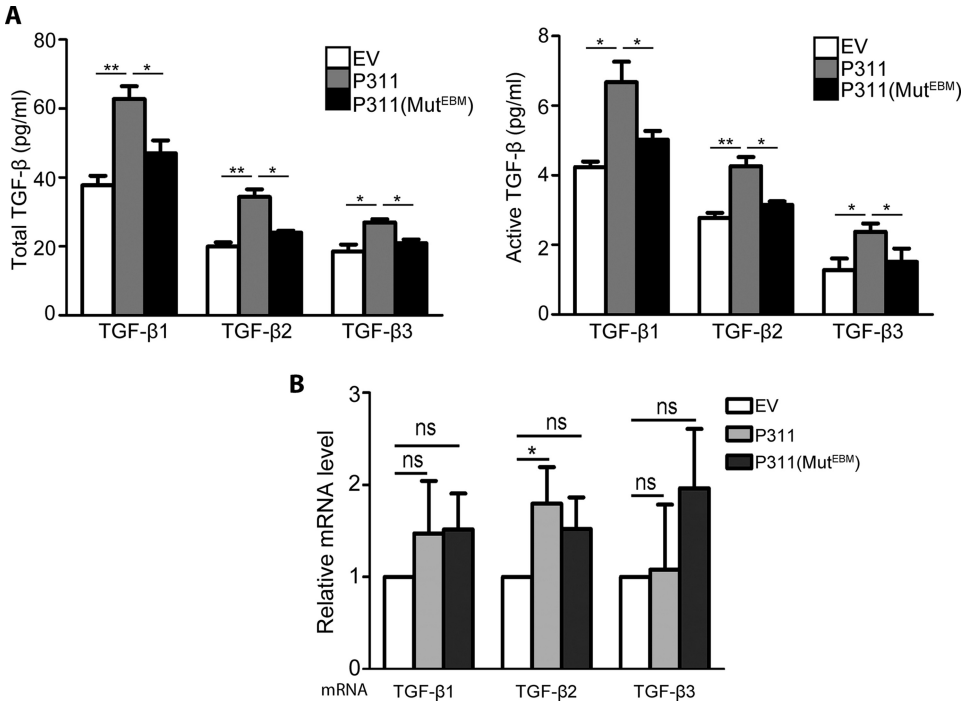

FIGURE 5. **The P311 EBM is required to stimulate a P311-mediated increase in TGF-βs in HLSMCs.** *A*, ELISA showing levels of total and active TGF-βs in the culture medium of human HLSMCs transfected with EV, P311, or P311(Mut^{EBM}). *, $p < 0.05$; **, $p < 0.01$. *B*, RT-qPCR analysis of the levels of TGF-β1-3 mRNAs in HLSMCs transfected with EV, P311, or P311(Mut^{EBM}). *, $p < 0.05$; *n.s.,* not significant.

It has been reported recently that eIF3b interacts with ribosomal proteins S9e, S3 and S14 (57, 58). In this regard, different ribosomal proteins, as well as several translation initiation factors, were inconsistently detected in P311 co-IP mass spectroscopy studies performed under low stringent conditions, but none was identified when the co-IP stringency was increased, rendering highly unlikely the possibility that ribosomal proteins and/or translation initiation factors others than eIF3b are direct P311 binding partners. Outside of the translation machinery, eIF3b interacts with the eukaryotic cytosolic chaperonin CCP (chaperonin-containing TCP-1 (tailless complex polypeptide 1)), which promotes the correct folding of the eIF3b, eIF3h, and eIF3i subunits (59). eIF3b interaction with the RNA-binding proteins AU-rich element RNA binding protein (AUF1) and ceramide kinase-like (CERKL) has also been observed recently (58, 60). None of these proteins were, however, identified in our co-IP mass spectroscopy studies.

SPR analysis indicated that the interaction between eIF3b and P311 has a higher affinity (K_d 1.26 μM) than the reported interaction between eIF3b and eIF3j (K_d 20 μM (36)). Therefore, P311 could, theoretically, displace eIF3j from the eIF3 complex. However, we observed no differences in eIF3b-eIF3j binding in the presence or absence of P311, and neither the composition nor the stoichiometry of the eIF3b-associated subcomplex (eIF3a, eIF3g, and eIF3i) (30) were affected. A new study determined the affinity of eIF3j to eIF3 at K_d 100 nM (61). This tight affinity supports our finding. Therefore, we ruled out the possibility that P311 may stimulate translation of TGF-β by producing qualitative and/or quantitative changes in the eIF3b-eIF3a-eIF3g-eIF3i subcomplex.

Structural studies have demonstrated previously that eIF3b folds into three independent domains (62). Its N-terminal domain contains an RRM (30, 36, 63), which, in mammalians, is non-canonical (63) but rather serves as the binding site for eIF3a (30), eIF3j (36), and P311 (our study). The N-terminal domain is connected with the central WD40 domain, which contains short, ~40-aa motifs often terminating in a WD, known as WD or β-transductin repeats. Proteins with WD40 repeats are known to serve as a platform for the assembly of protein complexes (64, 65). As such, the eIF3b WD40 domain interacts with the 40 S ribosomal subunit (57). This domain is followed by the C-terminal domain, necessary for the interaction with subunits eIF3i and eIF3g (47, 66). Mutational analysis suggests that P311 binding to eIF3b involves the RRM. This finding supports the possibility that eIF3b-bound P311 is located in close proximity to eIF3a and eIF3j. Our studies, however, revealed no P311 interaction or competition with either of them, indicating that the RRM region of eIF3b has multiple binding partners. RRM-containing genes represent about 0.5–1% of all human genes (67). Therefore, if the RRM represents the only P311 binding motif in the context of mRNA translation, the number of transcripts regulated by P311 should be relatively small. On the other hand, we identified the eIF3b binding region in P311 as a centrally located, 11-aa-long sequence (from leucine 30 to lysine 40), highly conserved among eukaryotic species, which we named EBM.

Systematic biochemical and functional studies demonstrated that EBM-mediated binding to eIF3b is required for P311 stimulation of TGF-β1-3 translation. The requirement of EBM-mediated P311-eIF3b interaction was confirmed by observing that expression of P311, but not P311(Mut^{EBM}), increased TGF-β1-3 levels in HLSMCs without increasing their corresponding mRNAs.

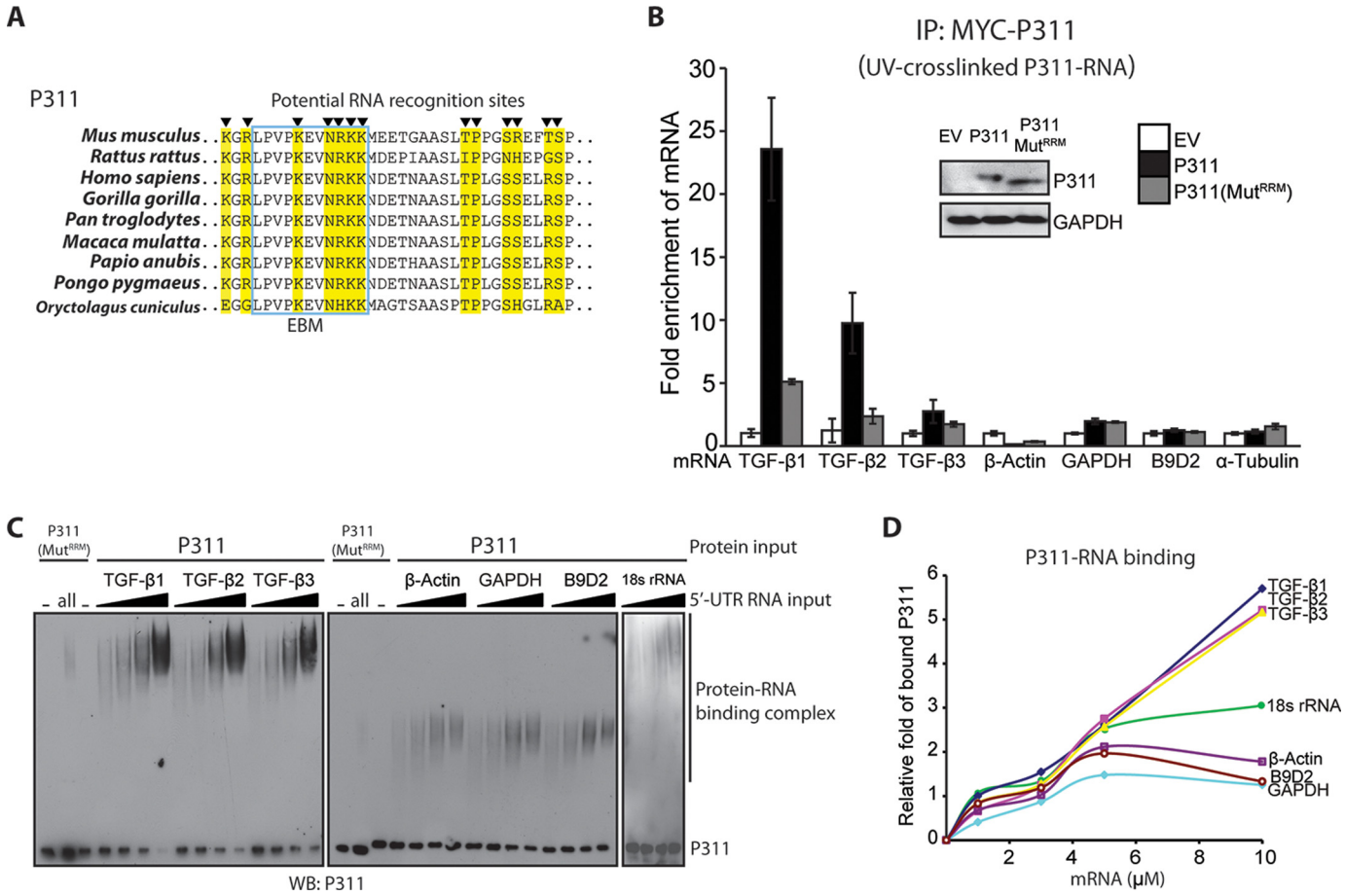

FIGURE 6. **P311 directly binds to the TGF-β1-3 5′UTRs through an RRM-like conserved aa signature.** *A*, predicted P311 RNA-binding sites (RRM-like) are shown in *yellow*, and the overlap with the P311 EBM is shown in a *blue box*. *B*, UV cross-linking followed by RIP assays showing enrichment in the 5′UTRs of TGF-β1-3 mRNAs in P311 IP from NIH-3T3 cells transfected with EV, P311, or P311(Mut^{RRM}). RNA enrichment was detected by RT-qPCR. *C*, protein-EMSA performed with purified P311 in the presence of increasing amounts (1, 3, 5, and 10 μM) of *in vitro*-translated mRNAs (*all*, a combined RNA sample (3 μM for each one) was added). After incubation, the proteins were resolved on a 4–20% Tris-glycine native gel, followed by Western blotting (*WB*) using P311 Ab. *D*, quantification of P311 RNA of the protein EMSA results.

The specific requirement for eIF3b in P311-mediated translation of mRNAs encoding TGF-β1-3 has been demonstrated in studies in which eIF3b or eIF3a control were down-regulated by RNAi in the presence or absence of P311. In such studies, P311 stimulated TGF-β translation when this was inhibited as a result of eIF3b down-regulation, but P311 had no effect on TGF-β translation when inhibited by down-regulation of eIF3a.

Although Blast and EMBL-EBI searches failed to identify distinct functional motifs in P311, a BindN search with 90% specificity (39) detected 13 potential RNA-binding residues distributed throughout its length, opening the possibility that P311 may bind RNA. Our *in vivo* and *in vitro* studies demonstrated that, indeed, P311 directly binds to TGF-β mRNAs but not to other mRNA controls. The binding was reduced significantly when substituting P311 for P311(Mut^{RRM}).

Western blot and RIP assays performed on material obtained from a single HA-eIF3b co-IP contained P311 as well as increased levels of TGF-β mRNAs compared with the samples obtained from P311(Mut^{EBM})- and empty vector-transfected cells, suggesting that P311 interaction with eIF3b and TGF-β 5′UTRs is concomitant. Altogether, these studies ruled out the possibility that P311 may stimulate translation of TGF-βs through its interaction with the cytoskeletal proteins identified in the co-IP-mass spectrometry studies because, in such a case, the effect on translation would be global.

During the process of translation initiation, several eIF3 subunits interact with RNA. The subunit eIF3j directly binds to the 40 S ribosomal RNA (68), and the subunits eIF3a, eIF3c, and eIF3d physically interact with the 5′UTRs of mRNAs (69–72). Therefore, one or more of these subunits is likely to interact with TGF-β 5′UTRs, explaining why translation of TGF-βs is not completely shut down in the absence of P311 (1).

As mentioned above, two mRNA-binding proteins, AUF1 and CERKL, also interact with eIF3b. AUF1 binding with eIF3b, along with S6 and S14, promotes the circadian translation of cryptochrome (58), and although the normal CERKL binds to eIF3b, the C125W CERKL, a pathological mutant that causes retinitis pigmentosa and cone-rod dystrophy, loses its interaction with eIF3b (60). To date, however, no other mRNA binding protein has been shown to display activities similar to that we now ascribe to P311.

In conclusion, our findings indicate that, by concomitantly binding to eIF3b through its EBM and to the 5′UTR of TGF-β1-3 mRNAs through its RRM, P311 recruits TGF-β1-3 mRNAs to the translation machinery, which, in turn, leads to

increased translation of TGF-βs and to the up-regulation of TGF-β1-3 levels.

REFERENCES

1. Badri, K. R., Yue, M., Carretero, O. A., Aramgam, S. L., Cao, J., Sharkady, S., Kim, G. H., Taylor, G. A., Byron, K. L., and Schuger, L. (2013) Blood pressure homeostasis is maintained by a P311-TGF-β axis. *J. Clin. Invest.* **123,** 4502–4512
2. Studler, J. M., Glowinski, J., and Lévi-Strauss, M. (1993) An abundant mRNA of the embryonic brain persists at a high level in cerebellum, hippocampus and olfactory bulb during adulthood. *Eur. J. Neurosci.* **5,** 614–623
3. Pan, D., Zhe, X., Jakkaraju, S., Taylor, G. A., and Schuger, L. (2002) P311 induces a TGF-β1-independent, nonfibrogenic myofibroblast phenotype. *J. Clin. Invest.* **110,** 1349–1358
4. Fujitani, M., Yamagishi, S., Che, Y. H., Hata, K., Kubo, T., Ino, H., Tohyama, M., and Yamashita, T. (2004) P311 accelerates nerve regeneration of the axotomized facial nerve. *J. Neurochem.* **91,** 737–744
5. Zhao, L., Leung, J. K., Yamamoto, H., Goswami, S., Kheradmand, F., and Vu, T. H. (2006) Identification of P311 as a potential gene regulating alveolar generation. *Am. J. Respir. Cell Mol. Biol.* **35,** 48–54
6. Tan, J., Peng, X., Luo, G., Ma, B., Cao, C., He, W., Yuan, S., Li, S., Wilkins, J. A., and Wu, J. (2010) Investigating the role of P311 in the hypertrophic scar. *PLoS ONE* **5,** e9995
7. Mariani, L., McDonough, W. S., Hoelzinger, D. B., Beaudry, C., Kaczmarek, E., Coons, S. W., Giese, A., Moghaddam, M., Seiler, R. W., and Berens, M. E. (2001) Identification and validation of P311 as a glioblastoma invasion gene using laser capture microdissection. *Cancer Res.* **61,** 4190–4196
8. Shi, J., Badri, K. R., Choudhury, R., and Schuger, L. (2006) P311-induced myofibroblasts exhibit ameboid-like migration through RalA activation. *Exp. Cell Res.* **312,** 3432–3442
9. Taylor, G. A., Rodriguiz, R. M., Greene, R. I., Daniell, X., Henry, S. C., Crooks, K. R., Kotloski, R., Tessarollo, L., Phillips, L. E., and Wetsel, W. C. (2008) Behavioral characterization of P311 knockout mice. *Genes Brain Behav.* **7,** 786–795
10. Sun, Y. G., Gao, Y. J., Zhao, Z. Q., Huang, B., Yin, J., Taylor, G. A., and Chen, Z. F. (2008) Involvement of P311 in the affective, but not in the sensory component of pain. *Mol. Pain* **4,** 23
11. Jenkins, R. H., Bennagi, R., Martin, J., Phillips, A. O., Redman, J. E., and Fraser, D. J. (2010) A conserved stem loop motif in the 5′untranslated region regulates transforming growth factor-β(1) translation. *PLoS ONE* **5,** e12283
12. Lyabin, D. N., Eliseeva, I. A., and Ovchinnikov, L. P. (2014) YB-1 protein: functions and regulation. *Wiley Interdiscip. Rev. RNA* **5,** 95–110
13. Fraser, D. J., Phillips, A. O., Zhang, X., van Roeyen, C. R., Muehlenberg, P., En-Nia, A., and Mertens, P. R. (2008) Y-box protein-1 controls transforming growth factor-β1 translation in proximal tubular cells. *Kidney Int.* **73,** 724–732
14. Martin, J., Jenkins, R. H., Bennagi, R., Krupa, A., Phillips, A. O., Bowen, T., and Fraser, D. J. (2011) Post-transcriptional regulation of transforming growth factor β-1 by microRNA-744. *PLoS ONE* **6,** e25044
15. Wang, B., Koh, P., Winbanks, C., Coughlan, M. T., McClelland, A., Watson, A., Jandeleit-Dahm, K., Burns, W. C., Thomas, M. C., Cooper, M. E., and Kantharidis, P. (2011) miR-200a prevents renal fibrogenesis through repression of TGF-β2 expression. *Diabetes* **60,** 280–287
16. Wu, C. Y., Tsai, Y. P., Wu, M. Z., Teng, S. C., and Wu, K. J. (2012) Epigenetic reprogramming and post-transcriptional regulation during the epithelial-mesenchymal transition. *Trends Genet.* **28,** 454–463
17. Meng, X. M., Chung, A. C., and Lan, H. Y. (2013) Role of the TGF-β/BMP-7/Smad pathways in renal diseases. *Clin. Sci.* **124,** 243–254
18. Wrzesinski, S. H., Wan, Y. Y., and Flavell, R. A. (2007) Transforming growth factor-β and the immune response: implications for anticancer therapy. *Clin. Cancer Res.* **13,** 5262–5270
19. Li, M. O., Wan, Y. Y., Sanjabi, S., Robertson, A. K., and Flavell, R. A. (2006) Transforming growth factor-beta regulation of immune responses. *Annu. Rev. Immunol.* **24,** 99–146
20. Massagué, J. (2008) TGFβ in cancer. *Cell* **134,** 215–230
21. Bierie, B., and Moses, H. L. (2006) TGF-β and cancer. *Cytokine Growth Factor Rev.* **17,** 29–40
22. Harvey, R. A., and Ferrier, D. R. (2011) *Biochemistry*, 5th ed., Wolters Kluwer Health/Lippincott Williams & Wilkins, Philadelphia
23. Silvera, D., Formenti, S. C., and Schneider, R. J. (2010) Translational control in cancer. *Nat. Rev. Cancer* **10,** 254–266
24. Alekhina, O. M., and Vassilenko, K. S. (2012) Translation initiation in eukaryotes: versatility of the scanning model. *Biochemistry* **77,** 1465–1477
25. Hinnebusch, A. G., and Lorsch, J. R. (2012) The mechanism of eukaryotic translation initiation: new insights and challenges. *Cold Spring Harb. Perspect. Biol.* **4,** a011544
26. Lomakin, I. B., and Steitz, T. A. (2013) The initiation of mammalian protein synthesis and mRNA scanning mechanism. *Nature* **500,** 307–311
27. Damoc, E., Fraser, C. S., Zhou, M., Videler, H., Mayeur, G. L., Hershey, J. W., Doudna, J. A., Robinson, C. V., and Leary, J. A. (2007) Structural characterization of the human eukaryotic initiation factor 3 protein complex by mass spectrometry. *Mol. Cell Proteomics* **6,** 1135–1146
28. Sun, C., Todorovic, A., Querol-Audí, J., Bai, Y., Villa, N., Snyder, M., Ashchyan, J., Lewis, C. S., Hartland, A., Gradia, S., Fraser, C. S., Doudna, J. A., Nogales, E., and Cate, J. H. (2011) Functional reconstitution of human eukaryotic translation initiation factor 3 (eIF3). *Proc. Natl. Acad. Sci. U.S.A.* **108,** 20473–20478
29. Masutani, M., Sonenberg, N., Yokoyama, S., and Imataka, H. (2007) Reconstitution reveals the functional core of mammalian eIF3. *EMBO J.* **26,** 3373–3383
30. Dong, Z., Qi, J., Peng, H., Liu, J., and Zhang, J. T. (2013) Spectrin domain of eukaryotic initiation factor 3a is the docking site for formation of the a:b:i:g subcomplex. *J. Biol. Chem.* **288,** 27951–27959
31. Hinnebusch, A. G. (2014) The scanning mechanism of eukaryotic translation initiation. *Annu. Rev. Biochem.* **83,** 779–812
32. Fraser, C. S., Berry, K. E., Hershey, J. W., and Doudna, J. A. (2007) eIF3j is located in the decoding center of the human 40S ribosomal subunit. *Mol. Cell* **26,** 811–819
33. Bendak, K., Loughlin, F. E., Cheung, V., O'Connell, M. R., Crossley, M., and Mackay, J. P. (2012) A rapid method for assessing the RNA-binding potential of a protein. *Nucleic Acids Res.* **40,** e105
34. Li, X., Romero, P., Rani, M., Dunker, A. K., and Obradovic, Z. (1999) Predicting protein disorder for N-, C-, and internal regions. *Genome Inform. Ser. Workshop Genome Inform.* **10,** 30–40
35. Dyson, H. J., and Wright, P. E. (2005) Intrinsically unstructured proteins and their functions. *Nat. Rev. Mol. Cell Biol.* **6,** 197–208
36. ElAntak, L., Tzakos, A. G., Locker, N., and Lukavsky, P. J. (2007) Structure of eIF3b RNA recognition motif and its interaction with eIF3j: structural insights into the recruitment of eIF3b to the 40 S ribosomal subunit. *J. Biol. Chem.* **282,** 8165–8174
37. Fraser, C. S., Lee, J. Y., Mayeur, G. L., Bushell, M., Doudna, J. A., and Hershey, J. W. (2004) The j-subunit of human translation initiation factor eIF3 is required for the stable binding of eIF3 and its subcomplexes to 40 S ribosomal subunits *in vitro*. *J. Biol. Chem.* **279,** 8946–8956
38. Jerng, H. H., Kunjilwar, K., and Pfaffinger, P. J. (2005) Multiprotein assembly of Kv4.2, KChIP3 and DPP10 produces ternary channel complexes with ISA-like properties. *J. Physiol.* **568,** 767–788
39. Wang, L., and Brown, S. J. (2006) BindN: a web-based tool for efficient prediction of DNA and RNA binding sites in amino acid sequences. *Nucleic Acids Res.* **34,** W243–W248
40. Granneman, S., Kudla, G., Petfalski, E., and Tollervey, D. (2009) Identification of protein binding sites on U3 snoRNA and pre-rRNA by UV cross-linking and high-throughput analysis of cDNAs. *Proc. Natl. Acad. Sci. U.S.A.* **106,** 9613–9618
41. Morino, S., Hazama, H., Ozaki, M., Teraoka, Y., Shibata, S., Doi, M., Ueda, H., Ishida, T., and Uesugi, S. (1996) Analysis of the mRNA cap-binding ability of human eukaryotic initiation factor-4E by use of recombinant wild-type and mutant forms. *Eur. J. Biochem.* **239,** 597–601
42. Wendel, H. G., Silva, R. L., Malina, A., Mills, J. R., Zhu, H., Ueda, T., Watanabe-Fukunaga, R., Fukunaga, R., Teruya-Feldstein, J., Pelletier, J., and Lowe, S. W. (2007) Dissecting eIF4E action in tumorigenesis. *Genes Dev.* **21,** 3232–3237

43. Hinnebusch, A. G. (2006) eIF3: a versatile scaffold for translation initiation complexes. *Trends Biochem. Sci.* **31,** 553–562
44. McDonough, W. S., Tran, N. L., and Berens, M. E. (2005) Regulation of glioma cell migration by serine-phosphorylated P311. *Neoplasia* **7,** 862–872
45. Eliscovich, C., Buxbaum, A. R., Katz, Z. B., and Singer, R. H. (2013) mRNA on the move: the road to its biological destiny. *J. Biol. Chem.* **288,** 20361–20368
46. Paliwal, S., Shi, J., Dhru, U., Zhou, Y., and Schuger, L. (2004) P311 binds to the latency associated protein and downregulates the expression of TGF-β1 and TGF-β2. *Biochem. Biophys. Res. Commun.* **315,** 1104–1109
47. Herrmannová, A., Daujotyte, D., Yang, J. C., Cuchalová, L., Gorrec, F., Wagner, S., Dányi, I., Lukavsky, P. J., and Valásek, L. S. (2012) Structural analysis of an eIF3 subcomplex reveals conserved interactions required for a stable and proper translation pre-initiation complex assembly. *Nucleic Acids Res.* **40,** 2294–2311
48. Khoshnevis, S., Hauer, F., Milón, P., Stark, H., and Ficner, R. (2012) Novel insights into the architecture and protein interaction network of yeast eIF3. *RNA* **18,** 2306–2319
49. Shalev, A., Valásek, L., Pise-Masison, C. A., Radonovich, M., Phan, L., Clayton, J., He, H., Brady, J. N., Hinnebusch, A. G., and Asano, K. (2001) *Saccharomyces cerevisiae* protein Pci8p and human protein eIF3e/Int-6 interact with the eIF3 core complex by binding to cognate eIF3b subunits. *J. Biol. Chem.* **276,** 34948–34957
50. Alvarez, M., Altafaj, X., Aranda, S., and de la Luna, S. (2007) DYRK1A autophosphorylation on serine residue 520 modulates its kinase activity via 14-3-3 binding. *Mol. Biol. Cell* **18,** 1167–1178
51. Nielsen, K. H., Szamecz, B., Valásek, L., Jivotovskaya, A., Shin, B. S., and Hinnebusch, A. G. (2004) Functions of eIF3 downstream of 48S assembly impact AUG recognition and GCN4 translational control. *EMBO J.* **23,** 1166–1177
52. Wang, H., Ru, Y., Sanchez-Carbayo, M., Wang, X., Kieft, J. S., and Theodorescu, D. (2013) Translation initiation factor eIF3b expression in human cancer and its role in tumor growth and lung colonization. *Clin. Cancer Res.* **19,** 2850–2860
53. Wang, Z., Chen, J., Sun, J., Cui, Z., and Wu, H. (2012) RNA interference-mediated silencing of eukaryotic translation initiation factor 3, subunit B (EIF3B) gene expression inhibits proliferation of colon cancer cells. *World J. Surg. Oncol.* **10,** 119
54. Hershey, J. W. (2010) Regulation of protein synthesis and the role of eIF3 in cancer. *Braz. J. Med. Biol. Res.* **43,** 920–930
55. Liang, H., Ding, X., Zhou, C., Zhang, Y., Xu, M., Zhang, C., and Xu, L. (2012) Knockdown of eukaryotic translation initiation factors 3B (EIF3B) inhibits proliferation and promotes apoptosis in glioblastoma cells. *Neurol. Sci.* **33,** 1057–1062
56. Elantak, L., Wagner, S., Herrmannová, A., Karásková, M., Rutkai, E., Lukavsky, P. J., and Valásek, L. (2010) The indispensable N-terminal half of eIF3j/HCR1 cooperates with its structurally conserved binding partner eIF3b/PRT1-RRM and with eIF1A in stringent AUG selection. *J. Mol. Biol.* **396,** 1097–1116
57. Liu, Y., Neumann, P., Kuhle, B., Monecke, T., Schell, S., Chari, A., and Ficner, R. (2014) Translation initiation factor eIF3b contains a nine-bladed β-propeller and interacts with the 40 S ribosomal subunit. *Structure* **22,** 923–930
58. Lee, K. H., Kim, S. H., Kim, H. J., Kim, W., Lee, H. R., Jung, Y., Choi, J. H., Hong, K. Y., Jang, S. K., and Kim, K. T. (2014) AUF1 contributes to cryptochrome1 mRNA degradation and rhythmic translation. *Nucleic Acids Res.* **42,** 3590–3606
59. Roobol, A., Roobol, J., Carden, M. J., Smith, M. E., Hershey, J. W., Bastide, A., Knight, J. R., Willis, A. E., and Smales, C. M. (2014) The chaperonin CCT interacts with and mediates the correct folding and activity of three subunits of translation initiation factor eIF3: b, i and h. *Biochem. J.* **458,** 213–224
60. Fathinajafabadi, A., Pérez-Jiménez, E., Riera, M., Knecht, E., and Gonzàlez-Duarte, R. (2014) CERKL, a retinal disease gene, encodes an mRNA-binding protein that localizes in compact and untranslated mRNPs associated with microtubules. *PLoS ONE* **9,** e87898
61. Sokabe, M., and Fraser, C. S. (2014) Human eukaryotic initiation factor 2 (eIF2)-GTP-Met-tRNAi ternary complex and eIF3 stabilize the 43 S pre-initiation complex. *J. Biol. Chem.* **289,** 31827–31836
62. Marintchev, A., and Wagner, G. (2004) Translation initiation: structures, mechanisms and evolution. *Q. Rev. Biophys.* **37,** 197–284
63. Khoshnevis, S., Neumann, P., and Ficner, R. (2010) Crystal structure of the RNA recognition motif of yeast translation initiation factor eIF3b reveals differences to human eIF3b. *PLoS ONE* **5,** e12784
64. Li, D., and Roberts, R. (2001) WD-repeat proteins: structure characteristics, biological function, and their involvement in human diseases. *Cell Mol. Life Sci.* **58,** 2085–2097
65. Smith, T. F., Gaitatzes, C., Saxena, K., and Neer, E. J. (1999) The WD repeat: a common architecture for diverse functions. *Trends Biochem. Sci.* **24,** 181–185
66. Asano, K., Phan, L., Anderson, J., and Hinnebusch, A. G. (1998) Complex formation by all five homologues of mammalian translation initiation factor 3 subunits from yeast *Saccharomyces cerevisiae*. *J. Biol. Chem.* **273,** 18573–18585
67. Romanelli, M. G., Diani, E., and Lievens, P. M. (2013) New insights into functional roles of the polypyrimidine tract-binding protein. *Int. J. Mol. Sci.* **14,** 22906–22932
68. Querol-Audi, J., Sun, C., Vogan, J. M., Smith, M. D., Gu, Y., Cate, J. H., and Nogales, E. (2013) Architecture of human translation initiation factor 3. *Structure* **21,** 920–928
69. Khoshnevis, S., Gunisova, S., Vlckova, V., Kouba, T., Neumann, P., Beznoskova, P., Ficner, R., and Valasek, L. S. (2014) Structural integrity of the PCI domain of eIF3a/TIF32 is required for mRNA recruitment to the 43S pre-initiation complexes. *Nucleic Acids Res.* **42,** 4123–4139
70. Kouba, T., Rutkai, E., Karásková, M., and Valášek, L. (2012) The eIF3c/NIP1 PCI domain interacts with RNA and RACK1/ASC1 and promotes assembly of translation preinitiation complexes. *Nucleic Acids Res.* **40,** 2683–2699
71. Lindqvist, L., Imataka, H., and Pelletier, J. (2008) Cap-dependent eukaryotic initiation factor-mRNA interactions probed by cross-linking. *RNA* **14,** 960–969
72. Yin, J. Y., Dong, Z. Z., Liu, R. Y., Chen, J., Liu, Z. Q., and Zhang, J. T. (2013) Translational regulation of RPA2 via internal ribosomal entry site and by eIF3a. *Carcinogenesis* **34,** 1224–1231